EASR

Engineering and Applied Science Research

https://www.tci-thaijo.org/index.php/easr/index

Published by the Faculty of Engineering, Khon Kaen University, Thailand

Development of mathematical models for engine performance and emissions of the producer gas-diesel dual fuel mode using Response Surface Methodology

Monorom Rith*[1, 2] and Jose Bienvenido Manuel M. Biona[1, 3]

[1]Mechanical Engineering Department, De La Salle University, Taft Ave, Manila City, 1004 Metro Manila, Philippines
[2]Research and Innovation Center, Institute of Technology of Cambodia, Russian Conf. Blvd, Phnom Penh, Cambodia
[3]Enrique K. Razon Jr. Logistics Institute, De La Salle University, LTI Spine Road, Laguna Blvd, Biñan, Laguna 4024, Philippines

Received 20 March 2020
Revised 20 May 2020
Accepted 4 June 2020

Abstract

Gasification is a renewable technology used to convert agro-waste to combustible gas, called producer gas. The gas can partially replace diesel fuel, thereby increasing agro-waste exploitation and reducing fossil fuel demand. Many previous studies have focused on technical feasibility and improvement of engine performance and combustion characteristics using the approach of one factor at a time. This study developed the mathematical models of engine performance (i.e., specific diesel consumption (SDC), specific energy consumption (SEC), electricity-thermal efficiency (ETE)) and flue gas emissions for a dual producer gas-diesel engine using Response Surface Methodology (RSM). Three explanatory variables were considered, including diesel injection time (DIT), gas flow rate (Gas), and engine load (Load). The findings highlighted that all the developed models are significant, and only less than 0.05% that the models could occur due to noise. Gas is the most influential attribute of all the response variables, and the engine load was statistically significant for all the response variables (except the specific nitrogen oxide emission). The DIT factor affected the specific carbon monoxide and hydrocarbon emissions only. The interaction effects of Gas and Load on the SEC and specific carbon dioxide and carbon monoxide emissions were negatively significant. The interaction effect of Gas and DIT statistically influenced the specific hydrocarbon emission. The findings are informative for future studies of life cycle assessment, decision-making process, net energy analysis of biomass-based producer gas production, etc.

Keywords: Experimental design, Engine performance, Emissions, Dual fuel engine, Synthesis gas, Diesel genset

Nomenclature

α	Distance of an axial run from a center point
ABDC	After bottom dead center
ATDC	After top dead center
BBDC	Before bottom dead center
BTDC	Before top dead center
CO	Carbon monoxide
CO_2	Carbon dioxide
ETE	Electricity-thermal efficiency
DIT	Diesel injection timing
FCCD	Face-centered cubic design
Gas	Gas flow rate
g	Gram
HC	Hydrocarbon
K	Kelvin
kWe	Kilowatt in electrical power
kWth	Kilowatt in thermal power
Load	Engine load
NO_X	Nitrogen oxides
PG	Producer gas
R^2	R-squared
R^2 Adj	Adjusted R-squared
rpm	Revolutions per minute
RSM	Response surface methodology
RMSE	Root mean square error
SDC	Specific diesel consumption
SEC	Specific energy consumption
SSE	Sum of squared errors

1. Introduction

Gasification is a renewable technology that is applied to convert solid carbonaceous biomass to combustible gas, called syngas or producer gas, through the thermo-chemical process with the presence of an oxidation agent (e.g., steam, air, oxygen, or their mixture) [1-2]. This technology is not new, and it has been applied for over 180 years [2]. Gasification of agro-waste biomass can increase the capacity of waste exploitation and mitigate fossil fuel demand. The gasification efficiency ranges from 48.77% to 76.68% [1]. The efficiency variation is significantly attributed to physicochemical properties of biomass (e.g., biomass dimensions, density, and biomass carbon content) [3-5], specific designs of gasifiers (e.g., downdraft gasifier, updraft gasifier, throatless gasifier, and Imbert gasifier) [1-2, 6], gasification variables (e.g., gas production rate, biomass consumption rate, air-fuel ratio, and gasification temperature) [5, 7-11], and gas cleaning-cum-cooling elements (e.g., water

*Corresponding author.
Email address: rith_monorom@dlsu.edu.ph
doi: 10.14456/easr.2021.3

scrubber, water spray, cyclone filter, and heat exchanger) [12-14].

A gasifier can be coupled with a compression ignition (CI) engine [15-20] or a spark ignition (SI) engine [21-25] to replace diesel fuel partially or gasoline fully, respectively. The technical feasibility (e.g., engine performance, emissions, combustion characteristics) of the gasifier-engine system using various biomass types (i.e., charcoal, wood chip, coir-pith, sawdust, ground nutshell, bagasse, Jatropha seedcake, Jatropha shell, Jatropha seed) have been extensively studied [12, 15-17, 19-20, 26-35]. The producer gas could replace diesel fuel by 49% [12] up to 86% [36], and the gas and diesel are used as an inducted gaseous fuel and pilot fuel, respectively. The causes of varied diesel replacement rates are attributed to biomass property, specific gasifier design, oxidation agent type, oxidation agent flow rate, etc [1-2]. Biodiesel and vegetable oil can be used with producer gas to run a CI engine to replace 100% diesel fuel [15, 17, 26, 29-30]. However, the peak heat release rate occurred lower and later and the combustion is less complete for the dual producer gas-vegetable oil fuel and the dual producer gas-biodiesel fuel compared with the dual producer gas-diesel fuel [15, 17, 29]. Elevated combustion efficiency and reduced pollutant emissions of the dual biodiesel-producer gas could be taken place, subject to splitting pilot injection with a dwell ranging from 10 to 30 degrees of crank angle, combined with the first injection timing from 35 to 20 degrees before the top dead center (BTDC) [30]. Hydrogen can be added into producer gas to improve engine performance and combustion characteristics [37-40]. An increase in hydrogen content in producer gas enriches combustion characteristics, engine performance, and exhaust emissions (other than nitrogen oxide) [39]. The peak of the net heat release rate was found higher with inducting hydrogen content into the dual producer gas-diesel fuel [38]. Additionally, a mixture combination of producer gas (PG) = 60% and hydrogen (H_2) = 40%) was the most suited one for the combustion duration and ignition delay in good comparison with that of pure diesel operation [40]. Some existing studies intended to improve combustion characteristics by increasing the compression ratio [41] and liquid fuel injection pressure [42], applying pilot injection splitting [30, 43], and advancing the diesel injection timing [19]. The dual producer gas-diesel engine should not be operated at the maximum diesel replacement rate due to less efficient combustion and higher flue gas emissions [12]. The combustion characteristics (i.e., combustion pressure, net heat release rate, cumulative heat release) perform poorer with an increase in gas flow rate higher than 10 kg/h [19].

Some recent studies have applied statistical analysis and Artificial Intelligence algorithms to develop mathematical models of engine performance and emissions and optimize the engine operating parameters for biofuels, subject to the contributions in increasing computer power and the development of uncertainty analysis [44-45]. Very few studies have applied Response Surface Methodology (RSM) to minimize electricity generation costs, specific diesel consumption, and specific CO_2 emissions by taking into account gas flow rate, engine load, and diesel injection timing [46-47]. The optimum flow rate of producer gas for the dual producer gas-diesel fuel mode was roughly 10 kg/h [46-47]. The most recent studies applied Response Surface Methodology (RSM) to study the impact of some potential explanatory variables on some response variables [48-50]. Uslu and Celik [48] used i-amyl alcohol blended with gasoline fuel to run a spark-ignition engine and applied Artificial Neural Network (ANN) to predict the response variables of engine performance and exhaust emissions according to some explanatory variables (i.e., fuel blends, compression ratio, and engine speed) and the RSM to optimize suitable engine operating conditions. The most suitable operating conditions were highlighted with the i-amyl alcohol ratio of 15% at 8.31 CR and 2957.58 rpm engine speed. Similarly, Aydın et al. applied the same concept for the compression-ignition engine powered by diesel blended with biodiesel at various ratios, and the result highlighted that the overall desirability was achieved at a biodiesel ratio of 32% with 816 W engine load and 470 bar injection pressure [49]. Simsek and Uslu applied the RSM approach to optimize the engine operating parameters regarding the performance and emissions of the compression-ignition engine to run on diesel blended with biodiesel, and the most suitable operating conditions were found at 1485 W engine load and 216 bar injection pressure as well as a biodiesel ratio of 25.79% [50].

Based on the literature discussed above, most of the previous studies intend to improve the engine performance and combustion characteristics and minimize emissions of dual producer gas-diesel engines, but those previous studies are based on the approach of one factor at a time and use the volumetric unit of emissions. Very few studies have optimized the gas flow rate to offset specific diesel consumption, carbon dioxide (CO_2) emissions, and electricity generation cost. The most recent studies applied the RSM and ANN to investigate the combustion of biodiesel blended with diesel and i-amyl alcohol blended with gasoline.

Regarding the literature discussed above, the development of mathematical models of engine performance and emission characteristics for a dual producer gas-diesel engine has yet to be conducted. The development of mathematical models for engine performance and emissions of the producer-diesel dual fuel mode in terms of some potential variables using a statistical design approach is novel to fill the gaps in the body of knowledge of biomass-based producer gas exploitation.

This study developed mathematical models of engine performance output variables (i.e., specific diesel consumption, specific energy consumption, electrical-thermal efficiency) and emissions (i.e., CO_2, CO, HC, NO_X) taking into account diesel injection timing (DIT), producer gas flow rate (Gas), and engine load (Load). The DIT, gas flow rate, and engine load are attributes, sometimes called factors, independent variables, explanatory variables, or input variables. The RSM was applied to develop the models, and Jatropha seed was used as the feedstock of a gasifier-engine unit in our study. The RSM is a mathematical and statistical technique being useful to model and analyze output variables of interest influenced by explanatory variables [51]. This method can capture the curvature effect of continuous explanatory variables on output variables using the end-point design concept with a few numbers of center points [51]. The RSM-based models of dual producer gas-diesel engine performance and emissions are informative for future study of life cycle assessment of biomass-derived producer gas, cost-benefit analysis and environmental benefits of biomass exploitation, the decision-making process of biomass utilization, net energy analysis of biomass-based producer gas production, etc.

The remainder of the paper is structured as follows. The next section is the methodology of the study, including the experimental setup of a gasifier-engine system and the design of experiments based on the RSM approach. The penultimate section consists of the model estimation results and discussion. The last section concludes the modeling results and provides direction for future work.

2. Methodology

2.1 Experimental setup

The flowchart of the experimental setup is illustrated in Figure 1. The gasifier-engine system consists of a gasifier, a gas cleaning unit, and a diesel generator. The gasifier used in our study is a closed-top, throatless, downdraft gasifier. The basic specifications of the gasifier are listed in Table 1. The gas cleaning system is composed of a cyclone filter, a shell-tube heat exchanger, and a dried-bed filter. A KM 186F engine was used

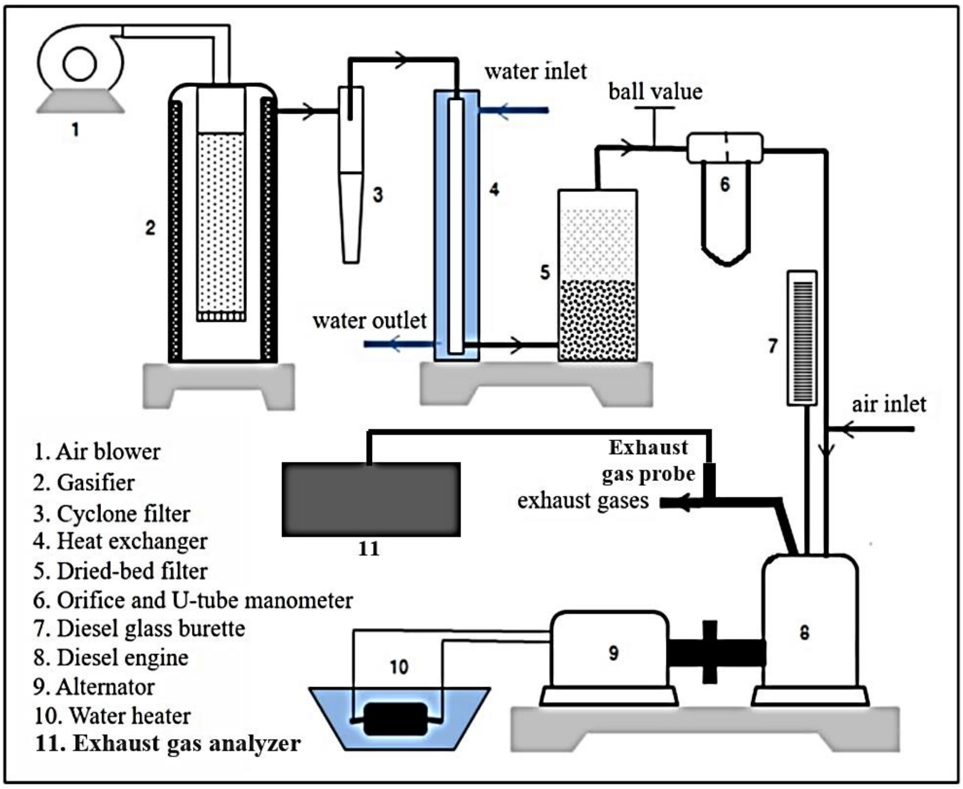

Figure 1 The schematic representation of the experimental set-up

Table 1 Gasifier specifications

Item	Description
Type	Closed top, throatless, downdraft
Gasifying agent	Air
The gasifier weight (kg)	30
Critical dimension (mm)	Diameter = 350 / height = 1800
Capacity (kWth)	130
Biomass consumption rate (kg/h)	5
Biomass type	Jatropha seed
Efficiency (%)	~77

Table 2 Engine specifications

Item	Description
Model	KM 186F
Engine type	Single cylinder, 4-stroke, air-cooled, direct injection, diesel engine
Bore×stroke (mm)	86×70
Connecting rod (mm)	117.5
Displacement (cm^3)	406
Rotational speed (rpm)	3,000
Compression ratio	19:1
Inlet valve	Open at an 8.5 degree BTDC, close at a 44.5 degree ABDC
Exhaust valve	Open at a 55.5 degree BBDC, close at an 8.5 degree ATDC
Rated output power (kW/rpm)	5.7/3,000

BTDC: Before top dead center
ABDC: After top dead center
BBDC: Before bottom dead center
ATDC: After top dead center

to operate on dual producer gas-diesel fuel mode, and its technical specifications are summarized in Table 2. The gas and air are mixed at the air filter box before entering the engine cylinder. A microprocessor tachometer with an accuracy of ±0.5 rpm of reading was used to read the engine speed. An MRU model exhaust gas analyzer with the measurement accuracy of ±5% for CO_2, ±12ppm for HC, ±0.06% for CO, and ±5ppm for NO_X was utilized to measure the flue gas concentrations (CO_2, CO, HC, and NO_X). An orifice and U-tube manometer were designed based on Bernoulli's principle to read producer gas flow rate. It assumes that the flow rate is non-compressible because of the inviscid, steady streamline. Water was used as the manometric fluid.

Jatropha seed was used as the feedstock for the gasifier. The seed is composed of 36.83% husk and 63.06% kernel [52] or contains 38% oil and 62% seedcake [53]. The dimensions of the seed is 21.02 mm (SD = ± 1.13) in length and 13.40 mm (SD = ± 0.36) in diameter [54]. The bulk density of the seed is 450 kg/m^3

Table 3 Producer gas properties [12]

Properties	Producer gas
H_2 (%)	12.50
CO (%)	17.50
CH_4 (%)	3.00
CO_2 (%)	15.00
N_2 (%)	52.00
Density (kg/m^3)	1.09
Calorific value (MJ/kg)	3.38

Table 4 Diesel fuel properties [17, 55]

Properties	Diesel fuel
Chemical Formula	$C_{13}H_{28}$
Cetane number	>50
Specific gravity	0.812
Kinematic viscosity (mm^2/s)	2.60
Calorific value (MJ/kg)	42.40
Flashpoint (°C)	52.00
Ignition temperature (°C)	240
Boiling temperature (°C)	160–370
Latent heat of evaporation (kJ/kg)	260

Table 5 Attributes and their levels

Attributes	Symbol	Variable Codes and levels		
Diesel injection timing	DIT (degree BTDC)	6	9	12
Gas flow rate	Gas (kg/h)	0	10	20
Engine load	Load (%)	35	52.5	70

BTDC: Before Top Dead Center

(SD = ± 10) [54]. The properties of the Jatropha seed are detailed in [52]. The Jatropha seed-derived gas was used to run the diesel engine in dual fuel mode. The properties of the producer gas and diesel are listed in Tables 3 and 4, respectively.

2.2 Response surface methodology (RSM)

The Face-Centered Cube Design (FCCD) technique of the RSM was applied to analyze the data because the region of the output variables (i.e., diesel consumption, energy consumption, electrical-thermal efficiency, flue gas emissions) are more likely to be cuboidal than spherical in shape. Furthermore, the FCCD allows the distance, α, of axial runs from the center points to be equal to 1, which allows the axial points located on the centers of the faces of the cube [51]. This is very convenient for our case study to control DIT (i.e., the lower and upper limits of the DIT are 6 degrees and 12 degrees before top dead center (BTDC), respectively, and therefore, the axial and center points of the DIT is 9 degrees BTDC). The FCCD does not require many center points, and only two or three center points are qualified to provide a good variance of prediction throughout the region of interest [51].

In our study, three attributes were considered, i.e., DIT, producer gas flow rate (Gas), engine load (Load). Their lower and upper levels are listed in Table 5. The JMP pro 12 software was used to analyze the experimental data. Based on the FCCD design of the experiment, three factors with two center points correspond to 16 experimental treatment combinations. Each treatment combination was performed in triplicate to ensure repeatability. The experimental data corresponding to experimental settings is tabulated in Table 6. There are seven output variables, i.e., specific diesel consumption (SDC), specific energy consumption (SEC), electrical-thermal efficiency (ETE), specific CO_2 emission (CO_2), specific CO emission (CO), specific HC emission (HC), specific NO_X emission (NO_X). The output variables of the designed treatment combinations are the average of three times of experiment to ensure repeatability, and the data in parentheses are the corresponding standard deviation values. The engine was operated at a high speed of 3,000 rpm for all the experimental settings. A comprehensive mathematical formulation is expressed as follows:

$$y_i = \beta_0 + (\beta_1\text{Gas}) + (\beta_2\text{Load}) + (\beta_3\text{DIT}) + (\beta_4 Gas^2) + (\beta_5 Load^2) + (\beta_6 DIT^2) + (\beta_7\text{Gas}\times\text{Load}) + (\beta_8\text{Gas}\times\text{DIT}) + (\beta_9\text{Load}\times\text{DIT}) + (\beta_{10}\text{Gas}^2\times\text{Load}) + (\beta_{11}\text{Gas}^2\times\text{DIT}) + (\beta_{12}\text{Load}^2\times\text{Gas}) + (\beta_{13}\text{Load}^2\times\text{DIT}) + (\beta_{14}\text{DIT}^2\times\text{Gas}) + (\beta_{15}\text{DIT}^2\times\text{Load}) \quad (1)$$

where y_i is a response variable type i, and β_j is a parameter estimate (j = 0, 1, …, 15).

3. Results and discussion

3.1 Model estimation results

The model estimation results of the response variables in terms of DIT, gas flow rate, and engine load are shown in Table 7. Only significant attributes at the 10% significant level are considered using the "Screening" function of JMP pro 12 software.

3.1.1 Summary of fit

R^2 value expresses the total variability of the response that could be explained by the attributes, and R^2 Adj value accounts for the number of significant terms in the model. R^2 and R^2 Adj close to 1 are preferable. The difference between R^2 and R^2 Adj less than 0.2 indicates that there is no problem with the model or data [51]. The different values between R^2 and R^2 Adj for all the seven models developed in our study are less than 0.2. Higher R^2 Adj value provides a better goodness-of-fit for regression models. The highest R^2 Adj value was found for the specific CO_2 emission model, followed by the specific energy consumption (SEC) model, the electrical-thermal efficiency (ETE) model, the specific diesel consumption (SDC) model, and the specific CO, HC, and NO_X emission models.

Table 6 Experimental results – an average of three times (standard deviation)

Attributes				Response Variables						
Run	**DIT (degree)**	**Gas (kg/h)**	**Load (%)**	**SDC (kg/kWeh)**	**SEC (MJ/kWeh)**	**ETE (%)**	**CO_2 (g/kWeh)**	**CO (g/kWeh)**	**HC (g/kWeh)**	**NO_X (g/kWeh)**
1	6	0	1	0.637 (0.02)	27.04 (1.15)	13.32 (0.56)	1978.32 (83.43)	20.8 (1.68)	1.91 (0.14)	11.31 (0.74)
2	6	0	2	0.432 (0.01)	18.32 (0.55)	19.65 (0.59)	1355.92 (41.4)	5.88 (0.17)	0.44 (0.01)	7.40 (0.22)
3	6	10	1.5	0.312 (0.01)	39.12 (0.21)	9.20 (0.05)	4440.22 (13.93)	182.83 (0.57)	49.45 (0.46)	15.59 (0.16)
4	6	20	1	0.363 (0.01)	93.02 (0.23)	3.87 (0.01)	10979.57 (25.68)	671.8 (12.14)	258.58 (1.57)	56.8 (0.65)
5	6	20	2	0.222 (0.01)	48.22 (0.14)	7.46 (0.02)	5990.03 (9.82)	223.87 (0.36)	63.89 (0.23)	41.08 (0.34)
6	9	0	1.5	0.423 (0.01)	17.94 (0.10)	20.06 (0.12)	1318.77 (7.40)	9.50 (0.20)	1.49 (0.10)	5.67 (0.12)
7	9	10	1	0.333 (0.01)	52.93 (0.19)	6.80 (0.02)	5994.8 (3.70)	386.84 (4.74)	93.83 (1.86)	21.65 (0.68)
8	9	10	1.5	0.274 (0.01)	37.49 (0.25)	9.60 (0.06)	4306.41 (16.89)	197.11 (0.77)	45.88 (0.58)	25.69 (0.27)
9	9	10	1.5	0.265 (0.01)	37.12 (0.21)	9.69 (0.05)	4282.96 (17.24)	197.63 (2.31)	44.38 (0.17)	25.42 (0.29)
10	9	10	2	0.223 (0.01)	28.87 (0.24)	12.46 (0.10)	3362.57 (13.93)	117.13 (2.12)	25.13 (0.53)	24.55 (0.3)
11	9	20	1.5	0.261 (0.01)	62.82 (0.18)	5.73 (0.01)	7574.3 (39.5)	517.7 (17.24)	71.07 (0.72)	32.62 (0.88)
12	12	0	1	0.52 (0.02)	22.05 (0.93)	16.34 (0.68)	1611.89 (68.41)	14.65 (0.62)	3.22 (0.13)	9.10 (0.31)
13	12	0	2	0.441 (0.03)	18.74 (1.38)	19.27 (1.41)	1389.54 (102.35)	3.69 (0.36)	0.69 (0.06)	7.90 (0.83)
14	12	10	1.5	0.298 (0.01)	38.53 (0.33)	9.34 (0.08)	4097.01 (46.16)	445.97 (15.18)	11.28 (0.24)	21.12 (0.21)
15	12	20	1	0.316 (0.01)	91.01 (0.42)	3.95 (0.01)	11515.31 (42.39)	642.9 (9.33)	45.26 (1.32)	38.02 (0.97)
16	12	20	2	0.218 (0.01)	48.04 (0.20)	7.49 (0.03)	6239.21 (25.15)	152.02 (5.95)	13.99 (0.12)	20.97 (0.11)

3.1.2 ANOVA and lack of fit

All the developed models are significant at the 5% significant level. Of six regression models (i.e., other than the specific HC emission model), the p-values are less than 0.0001, which implies that there exists less than a 0.01% chance that the six models could occur due to noise. On the other hand, there is only a 0.05% chance that the specific HC emission model could occur due to noise. Lack of fit is used to assess how a model fits the data well, and a non-significant lack of fit is desirable. Of all the developed models, except the specific CO and HC emission models, the lack of fit is non-significant. Therefore, the developed specific CO and HC emission models cannot be used as the predictors of the response variables. That the lack-of-fit values of these two variables are statistically significant might be due to that the region of interest of these variables is spherical rather than cuboidal. Future studies might use the Spherical Central Composite Design (Spherical CCD) method in place of the FCCD method to develop the mathematical models of the specific CO and HC emissions for a dual producer gas-diesel fuel engine.

3.1.3 Parameter estimates

The parameter estimates of the seven models are listed in Table 7. The estimates of the developed models are the actual values, and the values in parentheses are the estimated standard errors. The intercept coefficients are included to capture the average unobserved effect.

The main effect (sometimes called linear effect) of gas flow rate is statistically significant for all the models, which implies that the gas flow rate affects the engine performance and emissions. The negative and positive signs indicate the inverse and direct effects of explanatory variables on response variables, respectively. The main effect of engine load statistically influenced all the output variables, other than the specific NO_X emission. This does not mean that the engine load does not affect the NO_X emission; on the other hand, the specific NO_X emission is mostly influenced by the gas flow rate relative to engine load. Similar studies have reported that the gas flow rate is the most significant factor of engine performance and emissions for the dual producer gas-diesel engine [34, 46-47, 56]. The DIT was statistically significant for the specific HC emission model only. The negative coefficient means that advancing the DIT is associated with reducing the HC emissions. Other previous studies also confirmed that HC emissions were reduced with a slightly advanced DIT [19, 39].

An interaction effect is the simultaneous effect of two or more attributes on a response variable, which tells an analyst how multiple attributes work together to impact one response variable. The interaction effects of gas with engine load on the SEC and specific CO_2 and CO emissions were significantly negative. This suggests that an increase in engine load is associated with reducing the SEC and specific CO_2 and CO emissions. This is inherent because fuel oxidation is more efficient at a higher engine load [2]. However, an increase in gas flow rate raises the three mentioned response variables because the coefficients of linear gas factors of the three response models are positive and higher than the corresponding interaction coefficients. These are consistent with the findings of the one-factor-at-a-time study of [28, 34, 56]. The interaction effect of Gas*DIT on the specific HC emission is significantly negative, which means that an

Table 7 Model estimation results – parameter estimate (standard error)

Term	SDC (kg/kWeh)	SEC (MJ/kWeh)	ETE (%)	CO_2 (g/kWeh)	CO (g/kWeh)	HC (g/kWeh)	NO_X (g/kWeh)
Parameter Estimates							
Intercept	0.283 (0.015)	37.60 (0.752)	9.518 (0.427)	4229.125 (91.857)	236.898 (18.529)	45.66 (7.224)	22.811 (1.859)
Gas	-0.107 (0.011)	23.901 (0.526)	-6.016 (0.33)	3127.76 (143.616)	215.38 (23.438)	44.505 (9.138)	14.811 (2.351)
Load	-0.064 (0.011)	-12.385 (0.526)	2.206 (0.33)	-1374.263 (64.227)	-123.442 (23.438)	-29.98 (9.138)	-
DIT	-	-	-	-	-	-29.867 (9.138)	-
Gas*Load	-	-9.465 (0.588)	-	-1177.609 (71.808)	-114.118 (26.204)	-	-
Gas*DIT	-	-	-	-	-	-33.095 (10.217)	-
Gas*Gas	0.099 (0.019)	3.727 (0.971)	2.199 (0.54)	322.47 (118.587)	-	-	-
Load*Load	-	4.247 (0.971)	-	554.62 (118.587)	-	-	-
Gas*Gas*DIT	-	-	-	-	-13.636 (26.204)	-	-
Load*Load*Gas	-	-	-	420.798 (160.567)	-	-27.745 (10.217)	-
Summary of Fit							
R^2	0.921158	0.996607	0.970268	0.997571	0.922761	0.863057	0.739103
R^2 Adj	0.901447	0.99491	0.962835	0.995951	0.894674	0.794586	0.720468
RMSE	0.037074	1.664606	1.046324	203.1037	74.11854	28.89953	7.437071
ANOVA and Lack of Fit							
Model	P-value: <.0001	P-value: <.0001	P-value: <.0001	P-value: <.0001	P-value: <.0001	P-value: 0.0005	P-value: <.0001
Lack of Fit	P-value: 0.4474	P-value: 0.3092	P-value: 0.1361	P-value: 0.4861	P-value: 0.0037	P-value: 0.0272	P-value: 0.8535

All the parameter estimates are statistically significant at the 10% level.

advancing DIT decreases the specific HC emission because the linear DIT factor of the specific HC emission is also significantly negative.

A quadratic effect is the interaction effect of one attribute with itself on one response variable. The quadratic producer gas factor was statistically significant for the SDC, SEC, ETE, and CO_2 emission models, which implied that those output variables were non-linear in terms of gas flow rate. Similar findings of the one-factor-at-a-time approach were reported in [28, 34, 56]. The quadratic effect of engine load on the SEC and specific CO_2 emission was significantly positive, and therefore, the SEC and specific CO_2 emission increased in a non-linear form with an increase in engine load. The same findings were found for the SEC [17, 27-28] and the specific CO_2 emission [16, 57].

Besides, the interaction term of the quadratic producer gas flow rate factor with the linear DIT factor negatively affected the specific CO emission. The interaction effects of the quadratic engine load factor with the linear gas factor were positive for the specific CO_2 emission and negative for the specific HC emission. These interaction terms are included to improve the model fit.

The developed models of SDC, SEC, ETE, CO_2, CO, HC, and NO_X are written as equations 2, 3, 4, 5, 6, 7, and 8, respectively, as follows.

$$SDC = 0.283 - (0.107\times Gas) - (0.064\times Load) + (0.099\times Gas^2) \quad (2)$$

$$SEC = 37.60 + (23.901\times Gas) - (12.385\times Load) - (9.465\times Gas\times Load) + (3.727\times Gas^2) + (4.247\times Load^2) \quad (3)$$

$$ETE = 9.518 - (6.016\times Gas) + (2.206\times Load) + (2.199\times Gas^2) \quad (4)$$

$$CO_2 = 4229.125 + (3127.76\times Gas) - (1374.263\times Load) - (1177.609\times Gas\times Load) + (322.47\times Gas^2) + (554.62\times Load^2) + (420.798\times Load^2\times Gas) \quad (5)$$

$$CO = 236.898 + (215.38\times Gas) - (123.442\times Load) - (114.118\times Gas\times Load) - (13.636\times Gas^2\times DIT) \quad (6)$$

$$HC = 45.66 + (44.505\times Gas) - (29.98\times Load) - (29.867\times DIT) - (33.095\times Gas\times DIT) - (27.745\ Load^2\times Gas) \quad (7)$$

$$NO_X = 22.811 + (14.811\times Gas) \quad (8)$$

The developed models are used to plot the response variables in terms of the attributes.

3.2 Surface plots of the developed models

3.2.1 Specific diesel consumption (SDC)

The surface plot of the SDC is illustrated in Figure 2. It was found that the SDC declined with an increased engine load due to better combustion at higher engine load and sharply fell off with an increase in gas flow rate. The same empirical finding was found [26, 33-34]. At high engine load, a further increase of producer gas more than 10 kg/h did not noticeably reduce the specific diesel consumption. Similar findings were empirically corroborated [33-34, 37], and other studies suggested that a dual producer gas-diesel engine is operated at a high load and not at the maximum diesel replacement rate [19, 46]. The optimum gas flow rate was 10 kg/h to make a trade-off between the specific

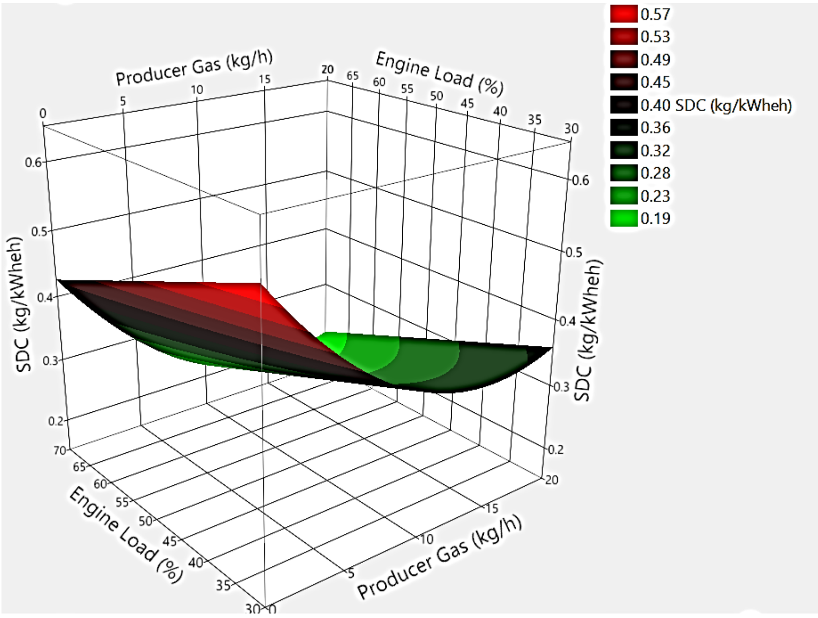

Figure 2 Specific diesel consumption (kg/kWeh)

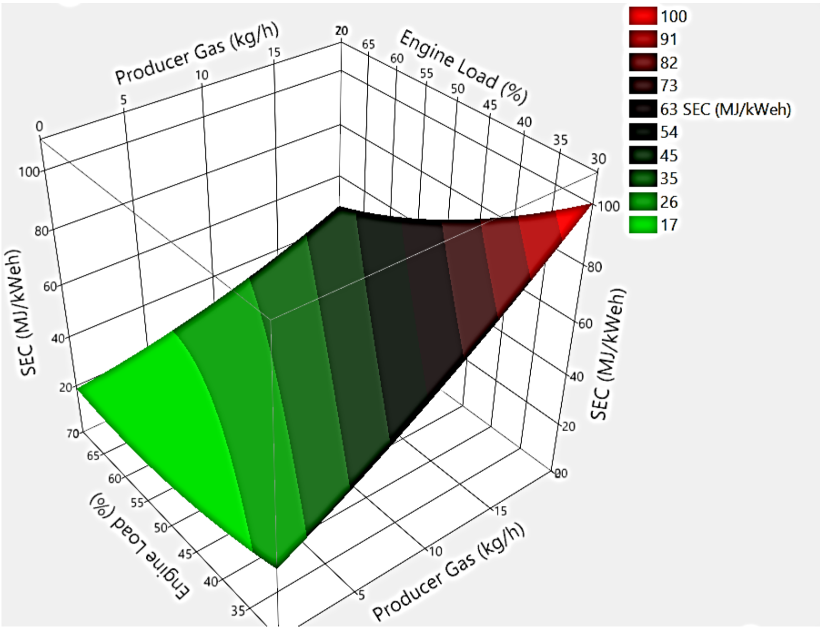

Figure 3 Specific energy consumption (MJ/kWeh)

diesel consumption and CO_2 emission [47]. It highlighted that the minimum SDC was 0.19 kg/kWeh when the engine was operated at 70% of the full engine load and the gas was controlled at a 10 kg/h flow rate.

3.2.2 Specific energy consumption (SEC)

Figure 3 depicts the surface plot of the SEC in terms of gas flow rate and engine load. The SEC rose steadily with an increase in gas flow rate, especially at low load. This implies that the combustion of dual producer gas-diesel fuel performs less efficiently with an increase in gas flow rate due to low-quality producer gas and restricted intake air for dual fuel combustion, which may narrow the effective flammability constraint [34]. The same finding was reported in the literature [27-28, 34]. However, at a 20 kg/h gas flow rate, the SEC suddenly declined from 100 MJ/kWeh at a 30% engine load to 45 MJ/kWeh at a 70% engine load. Correspondingly, the dual-fuel engine should be operated at a high engine load but not a high gas flow rate.

3.2.3 Electrical-thermal efficiency (ETE)

The ETE surface plot is illustrated in Figure 4. The maximum ETE was 20% at a high engine load with no gas. The ETE dramatically decreased when the engine was operated at a lower engine load and the gas flow rate increased. Similar findings of previous studies were confirmed [15, 29, 34]. At the maximum engine load, the ETE significantly declined to 14% at a 10 kg/h gas flow rate and 7% at a 20 kg/h gas flow rate. The lowest ETE was 3% when the engine was operated at a 35% engine load and a 20 kg/h gas flow rate. The dual-fuel oxidation, therefore, was less efficient at a high gas flow rate and low load. This can be explained that the combustion temperature is higher at a higher engine load [27, 32], thereby increasing reaction and oxidation rate [2, 47]. Furthermore, the less efficient combustion of dual producer gas-diesel fuel at a higher gas flow rate is due to the fact that the adiabatic flame temperature of producer gas was 1,730 K [58], which was much less than that of diesel fuel (2,325 K) [59].

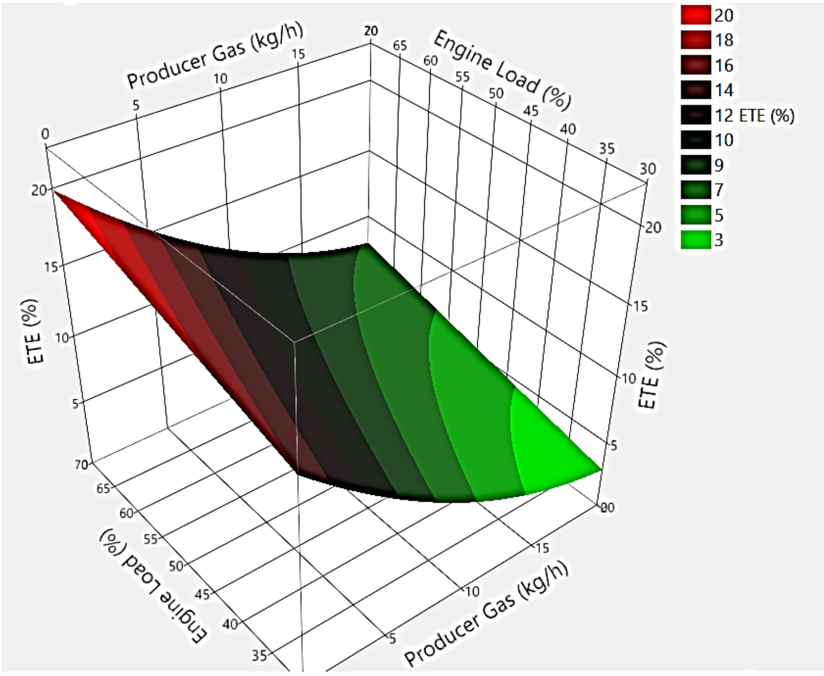

Figure 4 Electrical-thermal efficiency (%)

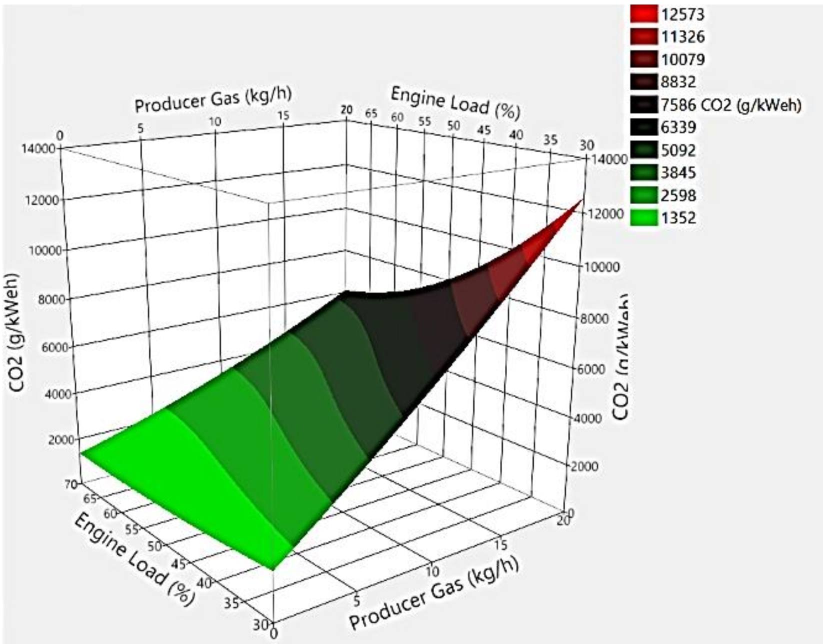

Figure 5 Specific CO_2 emission (g/kWeh)

Furthermore, the ignition center number is reduced as a result of an increase in gas flow rate, which leads to poorer fuel oxidation.

3.2.4 Specific CO_2 emission (g/kWeh)

The specific CO_2 emissions are viewed in the 3-D plot, as apparent in Figure 5. The specific CO_2 emissions were found lower at high engine load compared to low engine load as a result of more complete combustion. The combustion temperature increases with engine load [26, 28], which improves the fuel oxidization or chemical reaction rate. Furthermore, an increase in engine load is significantly associated with an increased pilot diesel fuel [26]. The specific CO_2 emissions shot up dramatically with an increase in the gas flow, especially at low load because of the already high presence of CO_2 constituent in producer gas [2]. The same finding was reported [47]. Consequently, the dual-fuel engine should be operated at the maximum engine load to mitigate the specific CO_2 emissions but not at the maximum gas flow rate. At the maximum engine load, the specific CO_2 emission doubled from 1,352 g/kWeh at no gas to 2,598 g/kWeh at a gas flow rate of 10 kg/h and jumped to 5,092 g/kWeh at a 20 kg/h gas flow rate.

3.2.5 Specific CO emission (g/kWeh)

The surface plots of specific CO emissions are apparent in Figure 6. The higher presence of CO emissions in flue gas concentration is an indication of less complete combustion. At a 20 kg/h gas flow rate and a 70% engine load, the specific CO emission slightly dropped off from 192 g/kWeh at the DIT of 6 degrees BTDC to 178 g/kWeh at the DIT of 9 degrees BTDC and further decreased to 164 g/kWeh at the DIT of 12 degrees BTDC. This elaborated that a marginal advanced DIT improved the dual

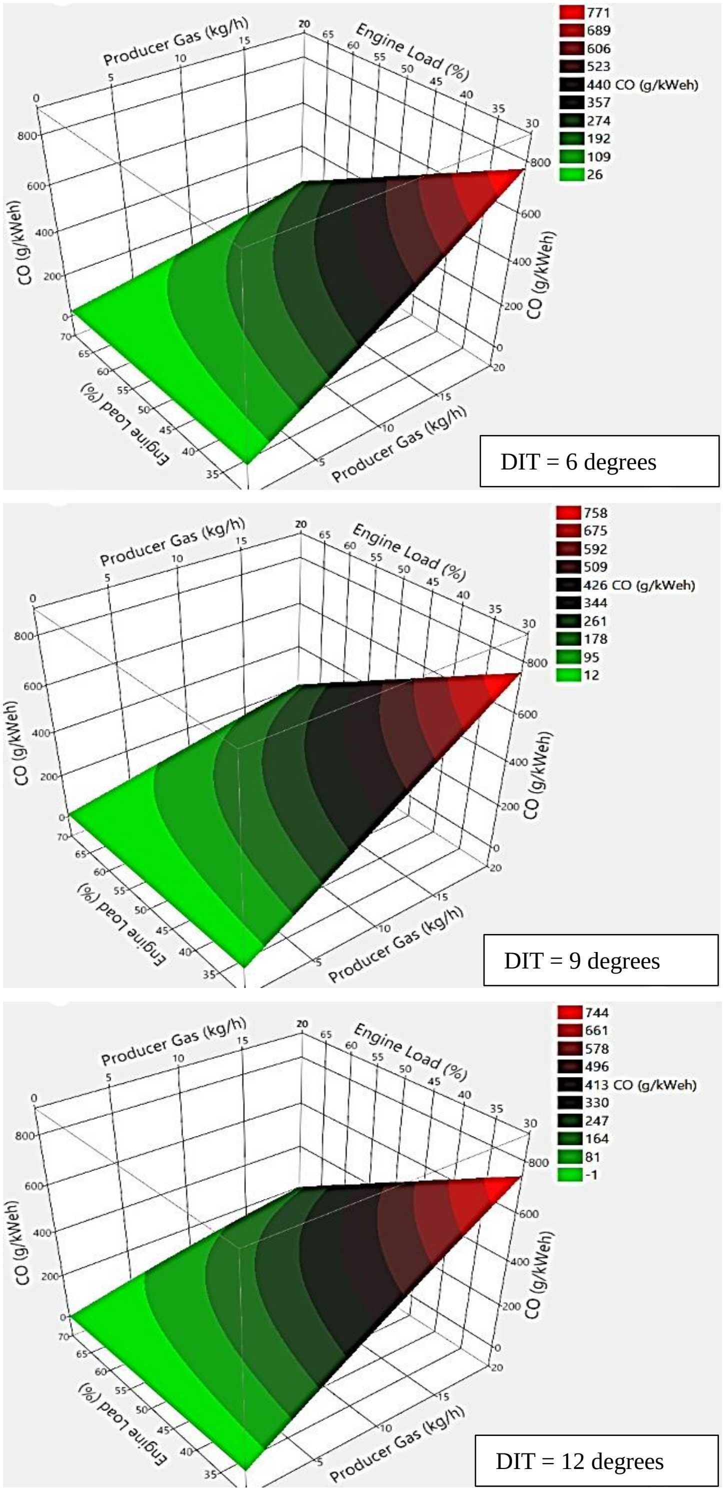

Figure 6 Specific CO emission (g/kWeh)

producer gas-diesel combustion because of advanced cumulative heat release during the premixed combustion, thereby increasing the chemical reaction rate [19]. The same finding was observed [39].

The specific CO emissions were found decidedly upwards with an increased gas flow rate. The same findings were observed [28, 34]. The already high presence of CO constituent in producer gas and less efficient combustion are the core reasons for the CO concentration in flue gas emissions [2]. Furthermore, the gaseous fuel is forced into the crevice volume of the cylinder during the compression stroke to escape fuel oxidation [60]. Additionally, an increase in gas flow rate inherently reduces the amount of pilot diesel, which provokes improper ignition timing, ignition delay, ignition duration, combustion duration, and degraded ignition centers [19, 34]. The peak of the net heat release rate of dual producer gas-diesel fuel occurred lower and later with an increase in gas flow rate [19, 35]. The CO emissions were dramatically reduced when the dual-fuel engine was operated at a higher engine load on account of more complete combustion. The dual producer gas-diesel engine should be operated at the maximum engine load [34, 47].

3.2.6 Specific HC emission (g/kWeh)

Figure 7 illustrates the surface plots of the specific HC emissions. The impact of DIT is more significant for the specific

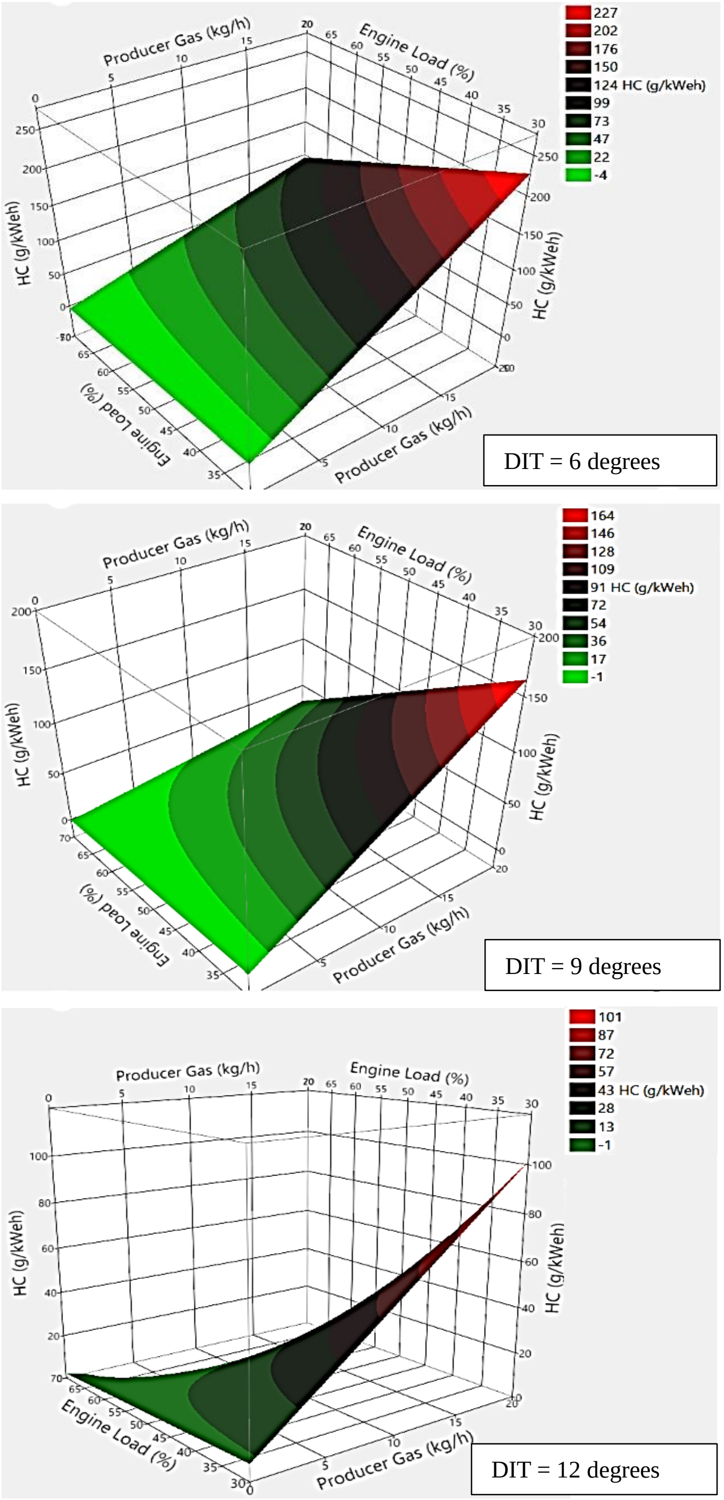

Figure 7 Specific HC emission (g/kWeh)

HC emissions relative to the specific CO emissions. As can be seen from the three plots of the figure, the specific HC emissions noticeably dropped off with a slightly advanced DIT at the highest engine load and gas flow rate. The same finding was reported [39]. At the 10 kg/h gas flow rate and high engine load, the specific HC emission declined from 47 g/kWeh at the DIT of 6 degrees BTDC to 17 g/kWeh at the DIT of 9 degrees BTDC. Advancing DIT caused a longer combustion duration that increased fuel oxidation duration [19]. However, the specific HC emissions are observed higher with an increased gas flow rate. This can be explained that an increase in gas flow rate is associated with the ignition delay period [19, 40, 61], and the delayed ignition duration is the main cause of higher HC emissions in a naturally aspirated direct-injection engine [29]. Additionally, this could be due to a lower air-fuel ratio and subsequently slower combustion with the escape of fuel from the combustion process [2]. The same finding was also found for the combustion of the dual biogas-diesel fuel [60].

At a high gas flow rate, the specific HC emissions significantly declined with an increase in engine load as a result of more complete combustion. An increase in engine load is associated with increased pilot diesel fuel that increases the ignition centers of dual-fuel combustion. Consequently, the ignition delay was reduced, the combustion duration was increased, and the cumulative heat release was found higher [19, 40].

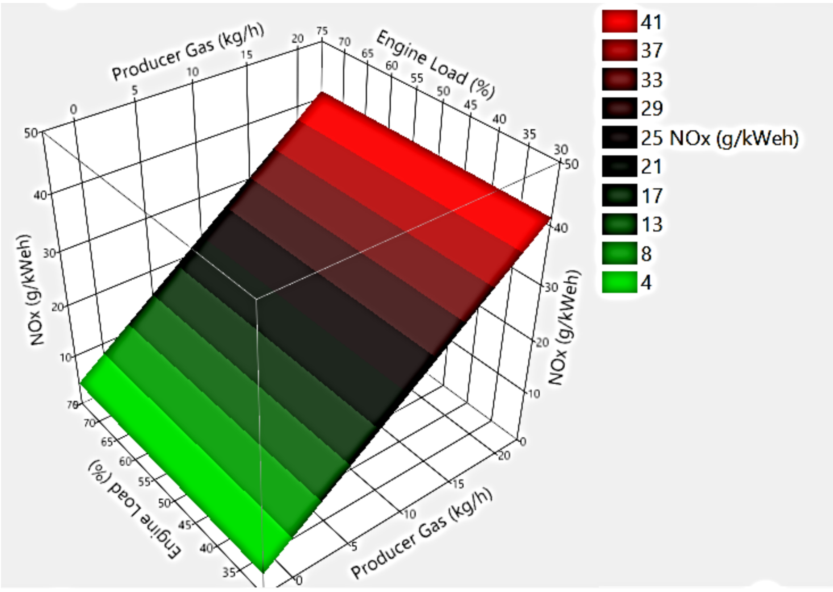

Figure 8 Specific NO_X emission (g/kWeh)

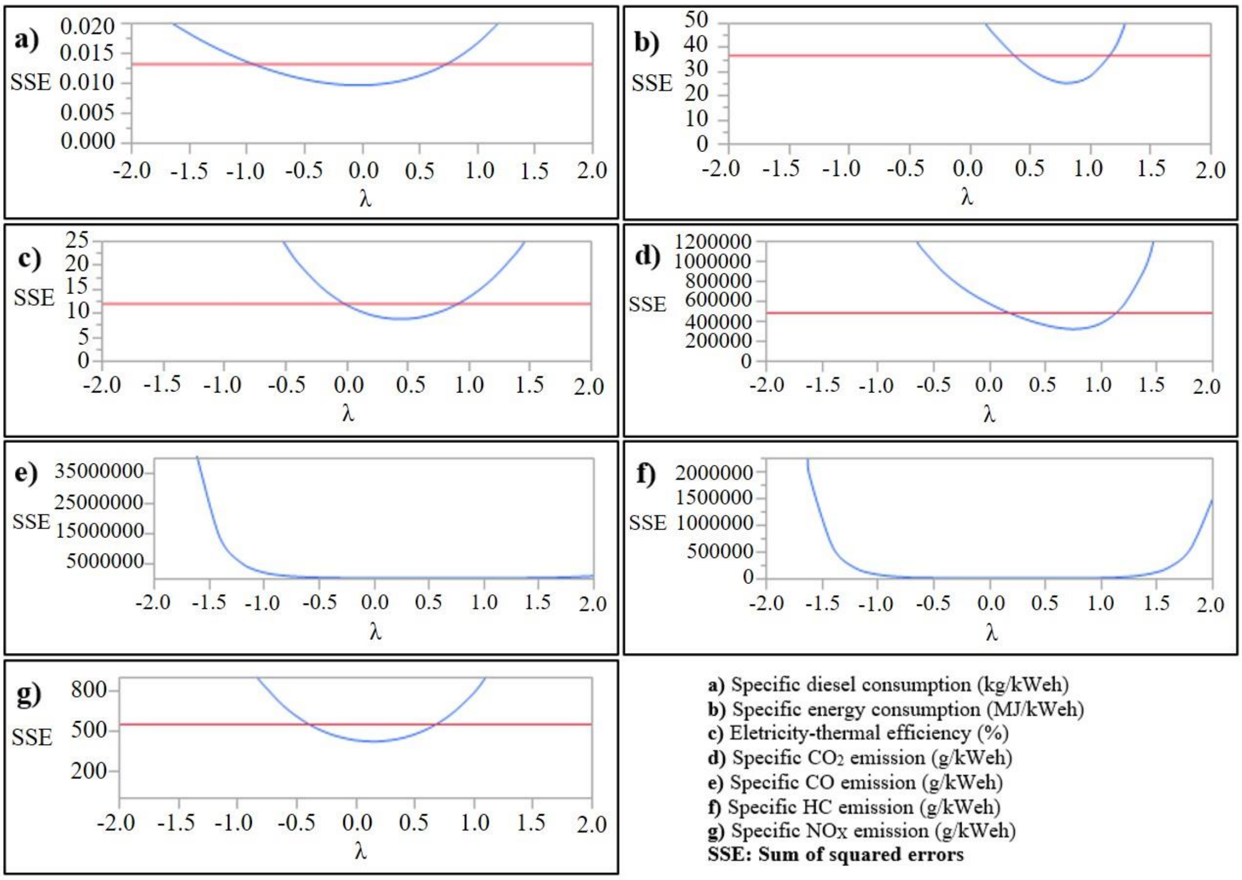

Figure 9 Box-Cox transformation graphs

3.2.7 Specific NO_X emission (g/kWeh)

The specific NO_X emissions in terms of engine load and gas flow rate are shown in Figure 8. Based on the statistical analysis, the engine load did not affect the specific NO_X emissions. This might be explained that the emission was mostly influenced by the gas flow rate because the gas flow rate interval was large (i.e., from zero to 20 kg/h gas flow rate), and the engine load has a much lower effect on the emissions, as compared to the gas flow. Another reason might be explained that the percentage change of NO_X emission was very comparable with that of engine load. The specific NO_X emissions linearly increased when the gas flow rate was increased from zero to 20 kg/h. The same findings were reported [19, 34]. Some reasons could be explained as follows. With an increase in gas flow rate, the cumulative heat release [19] and the exhaust temperature [27, 31-32] are observed higher, which implies a higher combustion temperature. Nitrogen is an inert gas at low temperatures, but it reacts with oxygen to form nitrogen oxides at high temperatures, specifically above 1,100 ℃ [62]. Another reason could be that the NO_X emissions in ppm

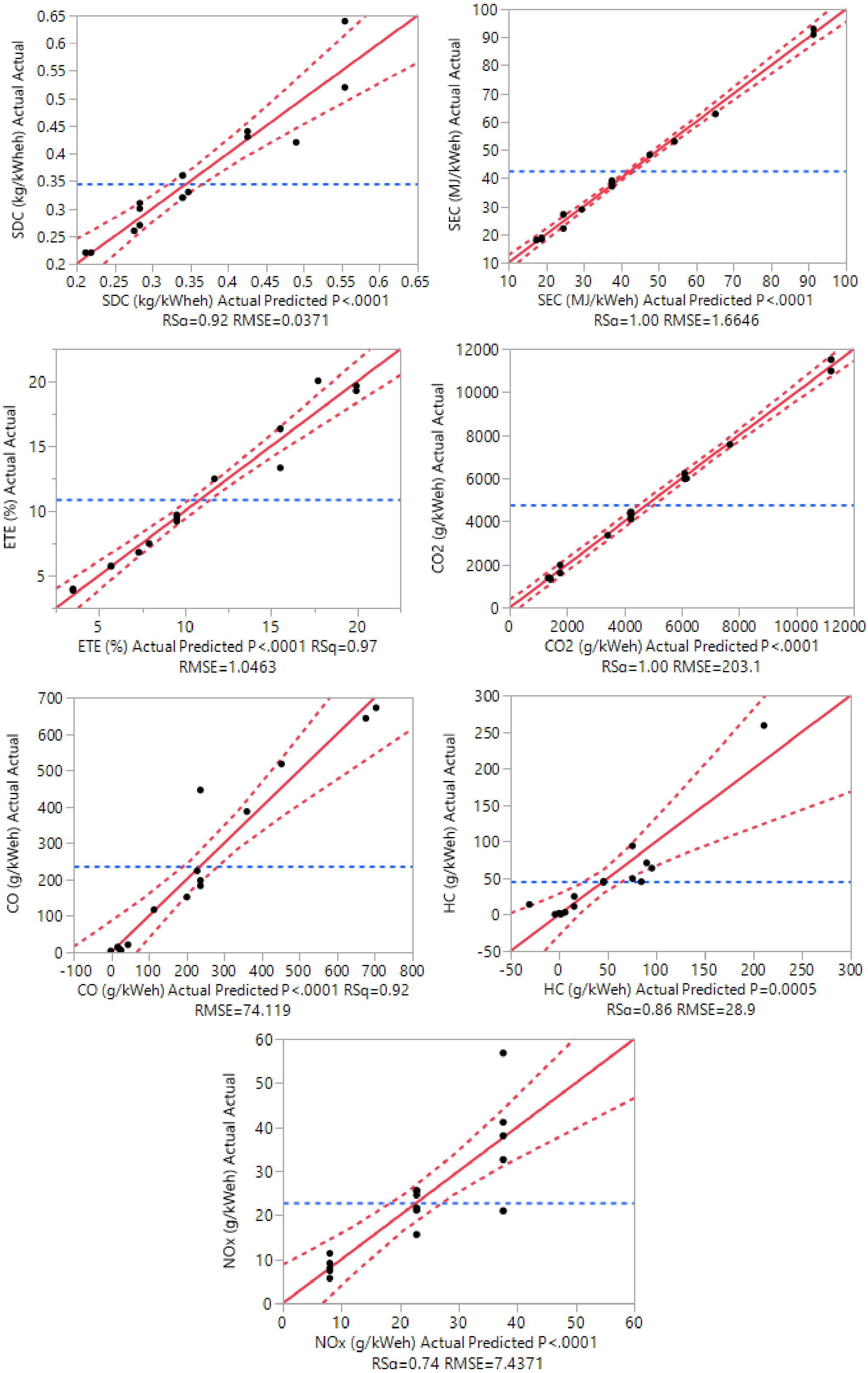

Figure 10 Actual by predicted plots

were lower at a higher gas flow [28], but the flue gas emission rate (e.g., m^3/h) was higher on account of higher gas flow rate (i.e., increase from zero to 20 kg/h), which can imply higher specific NO_X emissions. As evident from the figure, the specific NO_X emission increased from 4 g/kWeh to 41 g/kWeh when the gas flow was controlled from no gas and to 20 kg/h, respectively.

3.3 Graphic views of Box-Cox transformation

Many statistical tests are typically based on the assumption of normality thanks to its simplicity and mathematical tractability. However, the distributions of real data sets are generally not approximately normal. A Box-Cox transformation is an approach to transform a non-normal dependent variable into a normal shape. This technique allows analysts to check whether the normality assumption of the data set is reasonable and to identify the optimal transformation parameter, Lambda (λ). The graphic view of Box-Cox transformation for the response variables of our research is depicted in Figure 9. The assumption is that among all the transformations with Lambda values ranging from -2 to +2, the transformed data have the highest likelihood to be normally distributed for the response variables of SDC, SEC, and ETE and the specific CO_2 and NO_X emissions, other than the specific CO and HC emissions.

3.4 Actual by predicted plots

The actual by predicted plots provides a visual assessment of model fit that reflects variation due to random effects. The actual by predicted plots of the response variables are depicted in Figure 10. The plots show the observed values on Y-axis against the predicted values on X-axis. The black dots should be close to the fitted line and located inside the red dashed lines (confidence levels). Points that are vertically distant from the line represent possible outliers that can adversely affect the model fit.

4. Conclusions and recommendations

4.1 Conclusions

Most of the previous studies have focused on the technical feasibility of producer gas combustion in engines operated in the dual fuel mode using the approach of one factor at a time. Our study developed the mathematical models of engine performance (i.e., SDC, SEC, ETE) and emissions (i.e., CO_2, CO, HC, NO_X) as functions of DIT, engine load, and gas flow rate. All the developed models are significant and less than 0.05% that all the models could occur due to noise. The lack of fit was found non-significant for all the models, other than the specific CO and HC emission models. Consequently, the CO and HC emission models could not be used as the response predictors. The R^2 and R^2 Adj values were found higher than 0.9 for the SDC, SEC, ETE, and specific CO_2 emission models and 0.7 for CO, HC, and NO_X emissions. The difference between the R^2 and R^2 Adj was less than 0.2 for all the models. Therefore, there is no problem with the developed models and data. After that, the parameter estimates were statistically interpreted and concluded as follows. The main effect of the gas flow rate significantly influenced all the models of engine performance and emissions. Similarly, the main effect of engine load statistically influenced all the output variables (except the specific NO_X emission). The main effect of DIT was found statistically significant for the specific HC emission model only. The interaction effects of gas flow rate with engine load on the SEC and specific CO_2 and CO emissions were negatively significant at the 0.1 significant level. Also, the interaction effect of gas flow rate and DIT statistically influenced the specific HC emission. The quadratic producer gas factor was statistically significant for the SDC, SEC, ETE, and specific CO_2 emission models. The quadratic effect of engine load on the SEC and specific CO_2 emission was significantly positive. Additionally, the interaction term of the quadratic producer gas flow rate factor with the linear DIT factor indicated the negative impacts on the specific CO emission. The interaction effects of the quadratic engine load factor with the linear gas factor were positive for the specific CO_2 emission and negative for the specific HC emission. The developed models were also used to plot the response variables and the impacts of explanatory variables on the response variables were discussed.

The lowest SDC was 0.19 kg/kWeh when the engine was operated at 70% of the full engine load and the gas was controlled at a 10 kg/h flow rate. The dual producer gas-diesel engine should be operated at the maximum engine load but not at the maximum diesel replacement rate. The SEC and specific CO_2, CO, HC, and NO_X emissions were found higher with an increase in gas flow rate. However, an increase in engine load decreased these output variables.

4.2 Recommendations

The developed models are highly expected to be informative for future studies of life cycle assessment of biomass-derived producer gas, cost-benefit analysis of a gasifier-engine system, the decision-making process of biomass utilization, net energy analysis of biomass-based producer gas production, etc. Future studies can also apply this concept for other biomasses (e.g., rice husk, woodchip, and cashew nutshell), biofuels (e.g., biodiesel, methanol, ethanol, and biogas), and internal combustion engines (e.g., spark-ignition engine and gas turbine) using other methods of design of experiments (e.g., fractional factorial design, orthogonal design, and Taguchi).

5. Acknowledgments

The authors are greatly indebted to three anonymous reviewers for critical reading and helpful comments on the first draft of the research paper. The authors appreciate the reviewers for their immense knowledge and voluntary efforts. This work received a research grant from the Japan International Cooperation Agency (JICA) under the AUN/SEED-Net Project for a Master's Degree program at De La Salle University, Philippines.

6. References

[1] Martínez JD, Mahkamov K, Andrade RV, Silva Lora EE. Syngas production in downdraft biomass gasifiers and its application using internal combustion engines. Renew Energ. 2012;38(1):1-9.
[2] Yaliwal VS, Banapurmath NR, Gireesh NM, Tewari PG. Production and utilization of renewable and sustainable gaseous fuel for power generation applications: A review of literature. Renew Sustain Energ Rev. 2014;34:608-27.
[3] Balu E, Chung JN. Bioresource Technology System characteristics and performance evaluation of a trailer-scale downdraft gasifier with different feedstock. Bioresour Technol. 2012;108:264-73.
[4] Erlich C, Fransson TH. Downdraft gasification of pellets made of wood, palm-oil residues respective bagasse: Experimental study. Appl Energ. 2011;88(3):899-908.
[5] Tinaut FV, Melgar A, Pérez JF, Horrillo A. Effect of biomass particle size and air superficial velocity on the gasification process in a downdraft fixed bed gasifier. An experimental and modelling study. Fuel Process Tech. 2008;89:1076-89.
[6] Jaojaruek K, Jarungthammachote S, Gratuito MKB, Wongsuwan H, Homhual S. Experimental study of wood downdraft gasification for an improved producer gas quality through an innovative two-stage air and premixed air / gas supply approach. Bioresour Technol. 2011;102:4834-40.
[7] Makwana JP, Pandey J, Mishra G. Improving the properties of producer gas using high temperature gasification of rice husk in a pilot scale fluidized bed gasifier (FBG). Renew Energ. 2019;130:943-51.
[8] Jain AK, Goss JR. Determination of reactor scaling factors for throatless rice husk gasifier. Biomass Bioenergy. 2000;18:249-56.
[9] Singh RN, Jena U, Patel JB, Sharma AM. Feasibility study of cashew nut shells as an open core gasifier feedstock. Renew Energ. 2006;31(4):481-7.
[10] Vyas DK, Singh RN. Feasibility study of Jatropha seed husk as an open core gasifier feedstock. Renew Energ. 2007;32(3):512-7.
[11] Patel B, Gami B, Bhimani H. Improved fuel characteristics of cotton stalk, prosopis and sugarcane bagasse through torrefaction. Energy Sustain Dev. 2011;15(4):372-5.

[12] Rith M, Buenconsejo B, Biona JBM. Design and fabrication of a downdraft gasifier coupled with a small-scale diesel engine. Eng Appl Sci Res. 2020;47(1):117-28.
[13] Reed TB, Das A. Handbook of Biomass Downdraft Gasifier Engine Systems. Washington: Government Printing Office; 1988.
[14] Hasler P, Nussbaumer T. Gas cleaning for IC engine applications from fixed bed biomass gasification. Biomass Bioenergy. 1999;16:385-95.
[15] Banapurmath NR, Tewari PG. Comparative performance studies of a 4-stroke CI engine operated on dual fuel mode with producer gas and Honge oil and its methyl ester (HOME) with and without carburetor. Renew Energ. 2009;34(4):1009-15.
[16] Sutheerasak E, Pirompugd W, Sanitjai S. Performance and emissions characteristics of a direct injection diesel engine from compressing producer gas in a dual fuel mode. Eng Appl Sci Res. 2018;45(1):47-55.
[17] Raheman H, Padhee D. Combustion characteristics of diesel engine using producer gas and blends of jatropha methyl ester with diesel in mixed fuel mode. Int J Renew Energ Dev. 2014;3(3):228-35.
[18] Rith M. Combustion effect of jatropha producer gas fumigation in a stationary diesel genset [MSc. Thesis]. Mechanical Engineering Department, De La Salle University; 2015. Available from: https://animorepository.dlsu.edu.ph/etd_masteral/4962/
[19] Rith M, Buenconsejo B, Gonzaga JA, Gitano-Briggs HW, Lopez NS, Biona JBM. The combustion and emission characteristics of the diesel engine operated on a dual producer gas-diesel fuel mode. Eng Appl Sci Res. 2019;46(4):360-70.
[20] Sutheerasak E, Pirompugd W, Sanitjai S. Investigation of supercharging producer gas in dual fuel mode on the performance and emissions of a diesel-engine generator. Int J Mater Mech Manuf. 2018;6(6):402-6.
[21] Maiti S, Bapat P, Das P, Ghosh PK. Feasibility study of jatropha shell gasification for captive power generation in biodiesel production process from whole dry fruits. Fuel. 2014;121:126-32.
[22] Nadaleti WC, Przybyla G. SI engine assessment using biogas , natural gas and syngas with different content of hydrogen for application in Brazilian rice industries: Efficiency and pollutant emissions. Int J Hydrogen Energ. 2018;43(21):10141-54.
[23] Arroyo J, Moreno F, Muñoz M, Monné C, Bernal N, Combustion behavior of a spark ignition engine fueled with synthetic gases derived from biogas. Fuel. 2014;117:50-8.
[24] Arroyo J, Moreno F, Munoz M, Monne C. Efficiency and emissions of a spark ignition engine fueled with synthetic gases obtained from catalytic decomposition of biogas. *Int* J Hydrogen Energ. 2013;38:3784-92.
[25] Homdoung N, Tippayawong N, Dussadee N. Prediction of small spark ignited engine performance using producer gas as fuel. Case Stud Therm Eng. 2015;5:98-103.
[26] Sutheerasak E, Pirompugd W, Ruengphrathuengsuka W, Sanitjai S. Comparative investigation of using DEB oil and supercharging syngas and DEB oil as a dual fuel in a DI diesel engine. Eng Appl Sci Res. 2019;46(1):26-36.
[27] Sombatwong P, Thaiyasuit P, Pianthong K. Effect of pilot fuel quantity on the performance and emission of a dual producer gas - Diesel engine. Energy Procedia. 2013;34:218-27.
[28] Shrivastava V, Jha AK, Wamankar AK, Murugan S. Performance and emission studies of a CI engine coupled with gasifier running in dual fuel mode. Procedia Eng. 2013;51:600-8.
[29] Banapurmath NR, Tewari PG, Yaliwal VS, Kambalimath S, Basavarajappa YH. Combustion characteristics of a 4-stroke CI engine operated on Honge oil, Neem and Rice Bran oils when directly injected and dual fuelled with producer gas induction. Renew Energ. 2009;34(7):1877-84.
[30] Carlucci AP, Ficarella A, Laforgia D, Strafella L. Improvement of dual-fuel biodiesel-producer gas engine performance acting on biodiesel injection parameters and strategy. Fuel. 2017;209:754-68.
[31] Ramadhas AS, Jayaraj S, Muraleedharan C. Dual fuel mode operation in diesel engines using renewable fuels: Rubber seed oil and coir-pith producer gas. Renew Energ. 2008;33(9):2077-83.
[32] Ramadhas AS, Jayaraj S, Muraleedharan C. Power generation using coir-pith and wood derived producer gas in diesel engines. Fuel Process Tech. 2006;87(10):849-53.
[33] Rith M, Biona JMB, Gitano–Briggs HW, Sok P, Gonzaga JA, Arbon N, et al. Performance and emission characteristics of the genset fuelled with dual producer gas – diesel. DLSU Research Congress 2016; 2016 Mar 7-9; Manila, Philippines. p. 1-7.
[34] Rith M, Gitano-Briggs HW, Arbon NA, Gonzaga JA, Biona JBM. The effect of Jatropha seed cake producer gas flow rates on a diesel engine operated on dual fuel mode at high engine speed. Eng Appl Sci Res. 2019;46(4):303-11.
[35] Rith M, Buenconsejo B, Gitano-Briggs HW, Biona JBM. Design and fabrication of a low-cost research facility for the study of combustion characteristics of a dual producer gas-diesel engine. Eng Appl Sci Res. 2020;47(4):447-57.
[36] Uma R, Kandpal TC, Kishore VVN. Emission characteristics of an electricity generation system in diesel alone and dual fuel modes. Biomass Bioenergy. 2004;27(2):195-203.
[37] Dhole AE, Yarasu RB, Lata DB, Priyam A. Effect on performance and emissions of a dual fuel diesel engine using hydrogen and producer gas as secondary fuels. Int J Hydrogen Energ. 2014;9:1-11.
[38] Dhole AE, Lata DB, Yarasu RB. Effect of hydrogen and producer gas as secondary fuels on combustion parameters of a dual fuel diesel engine. Appl Therm Eng. 2016;108:764-73.
[39] Roy MM, Tomita E, Kawahara N, Harada Y, Sakane A. Performance and emission comparison of a supercharged dual-fuel engine fueled by producer gases with varying hydrogen content. Int J Hydrogen Energ. 2009;34(18):7811-22.
[40] Dhole AE, Yarasu RB, Lata DB. Investigations on the combustion duration and ignition delay period of a dual fuel diesel engine with hydrogen and producer gas as secondary fuels. Appl Therm Eng. 2016;107:524-32.
[41] Lal S, Mohapatra SK. The effect of compression ratio on the performance and emission characteristics of a dual fuel diesel engine using biomass derived producer gas. Appl Therm Eng. 2017;119:63-72.
[42] Carlucci AP, Ficarella A, Laforgia D. Potentialities of a common rail injection system for the control of dual fuel biodiesel-producer gas combustion and emissions. J Energ Eng. 2014;140(3):1-8.
[43] Carlucci AP, Colangelo G, Ficarella A, Laforgia D, Strafella L. Improvements in dual-fuel biodiesel-producer gas combustion at low loads through pilot injection splitting. J Energ Eng. 2015;141(2):1-8.
[44] Hamdia KM, Ghasemi H, Zhuang X, Alajlan N, Rabczuk T. Sensitivity and uncertainty analysis for flexoelectric nanostructures. Comput Meth Appl Mech Eng. 2018;337:95-109.
[45] Vu-Bac N, Lahmer T, Zhuang X, Nguyen-Thoi T, Rabczuk T. A software framework for probabilistic sensitivity analysis for computationally expensive models. Adv Eng Software. 2016;100:19-31.
[46] Rith M, Gitano-Briggs HW, Gonzaga JA, Biona JBM, Optimization of control factors for a diesel engine fueled

with jatropha seed producer gas on dual fuel mode. Int Energ J. 2019;19(3):149-58.
[47] Rith M, Arbon NA, Biona JBM. Optimization of diesel injection timing, producer gas flow rate, and engine load for a diesel engine operated on dual fuel mode at a high engine speed. Eng Appl Sci Res. 2019;46(3):192-9.
[48] Uslu S, Celik MB. Performance and exhaust emission prediction of a si engine fueled with i-amyl alcohol-gasoline blends: an ann coupled rsm based optimization. Fuel. 2020;265:116922.
[49] Aydın M, Uslu S, Bahattin Çelik M. Performance and emission prediction of a compression ignition engine fueled with biodiesel-diesel blends: a combined application of ANN and RSM based optimization. Fuel. 2020;269:117472.
[50] Simsek S, Uslu S. Determination of a diesel engine operating parameters powered with canola, safflower and waste vegetable oil based biodiesel combination using response surface methodology (RSM). Fuel. 2020;270:117496.
[51] Montgomery DC. Design and Analysis of Experiments. 5th ed. New York: John Wiley & Sons; 2001.
[52] Achten WMJ, Verchot L, Franken YJ, Mathijs E, Singh VP, Aerts R, et al. Jatropha bio-diesel production and use. Biomass Bioenergy. 2008;32(12):1063-84.
[53] Pandey KK, Pragya N, Sahoo PK. Life cycle assessment of small-scale high-input Jatropha biodiesel production in India. Appl Energ. 2011;88(12):4831-9.
[54] Khalil HPSA, Aprilia NAS, Bhat AH, Jawaid M, Paridah MT, Rudi D. A Jatropha biomass as renewable materials for biocomposites and its applications. Renew Sustain Energ Rev. 2013;22:667-85.
[55] Uslu S, Celik MB. Prediction of engine emissions and performance with artificial neural networks in a single cylinder diesel engine using diethyl ether. Eng Sci Tech, Int J. 2018;21(6):1194-201.
[56] Rith M, Biona JBM, Maglaya AB, Fernando A, Gonzaga JA, Gitano-Briggs HW. Fumigation of producer gas in a diesel genset: Performance and emission characteristics. 2018 IEEE 10th International Conference on Humanoid, Nanotechnology, Information Technology, Communication and Control, Environment and Management; 2018 Nov 29 - Dec 2; Baguio City, Philippines. USA: IEEE; 2019. p. 1-4.
[57] Nayak SK, Mishra PC. Combustion characteristics, performances and emissions of a biodiesel-producer gas dual fuel engine with varied combustor geometry. Energy. 2019;168:585-600.
[58] Hernandez JJ, Barba J, Aranda G. Combustion characterization of producer gas from biomass gasification. Glob Nest J. 2012;14(2):125-32.
[59] Glaude PA, Fournet R, Bounaceur R, Molière M. Adiabatic flame temperature from biofuels and fossil fuels and derived effect on NOx emissions. Fuel Process Tech. 2010;91(2):229-35.
[60] Mustafi NN, Raine RR, Verhelst S. Combustion and emissions characteristics of a dual fuel engine operated on alternative gaseous fuels. Fuel. 2013;109:669-78.
[61] Banapurmath NR, Tewari PG, Hosmath RS. Experimental investigations of a four-stroke single cylinder direct injection diesel engine operated on dual fuel mode with producer gas as inducted fuel and Honge oil and its methyl ester (HOME) as injected fuels. Renew Energ. 2008;33(9):2007-2018.
[62] Mathur M, Sharma R. Internal Combustion Engine. India: Dhanpat rai publication; 2006.